UDC 621.373.122

# THEORY OF STABILIZED AUTODYNE OSCILLATORS AT THE LARGE REFLECTED SIGNAL

Vladislav Ya. Noskov[1], Kirill A. Ignatkov[1], Sergey M. Smolskiy[2]

[1]Ural Federal University (UPI), Ekaterinburg, Russia
[2]National Research University "Moscow Power Engineering Institute", Moscow, Russia

Research results on autodyne oscillator stabilized by an external high-*Q* cavity are presented for the case of the large reflected signal, when amplitude of the reflected wave is commensurable with amplitude of natural oscillations. Expressions describing an autodyne response of the oscillator on the influence of the proper radiation reflected from a target are obtained. Calculations of amplitude, frequency and spectral characteristics of the autodyne system are performed. Conditions of exact tuning of the stabilized cavity are determined. Investigations of stabilized autodyne parameters at small distance to the reflected object are provided. It is shown that to expand the dynamic range of the autodyne system it is expedient to use the large coupling between cavities. Recommendations concerning practical application of the obtained results in the short-range radar are given.

## Introduction

One of the most important problems for development of short-range radar (SRR) is a provision of their maximal dynamic range with respect to the input signal level. The solution of this problem is in the direct dependence upon operation effectiveness of the SRR autodyne system included in the SRR structure. The problem is complicated due to the variations in wide range of the effective scattering areas of targets as well as distances to reflected objects. In the real SRR operating conditions, these distances can be changed from the maximally possible distance to the target determined by the system's energy potential to direct contiguity of the tracking object and SRR [1–6]. In the first case, the level of reflected radiation is quite small and often commensurable with the intrinsic noise level of the receiver, while in the second case it is large and commensurable with the probing radiation level of the transmitter. In many applications, the duration of target presence in the SRR monitoring zone and time of receiving signal processing for command working-out are limited. In these cases, application of various automatic control devices to expand the system dynamic range becomes ineffective due to large response time.

Solution of the dynamic range expansion problem of the autodyne SRR of millimeter wavelength range, which have clearly observed signal distortions [7, 8] at reflected radiation level growth, have the special significance. The origin of these distortions has the principal character and is connected with the phase shift irregularity for the reflected wave due to autodyne variations of oscillation frequency under influence of reflected radiation [8–10]. These distortions are peculiar to both usual autodynes with non-modulated radiation and autodyne oscillators with different types of modulation [11–14]. In most cases, they disturb the normal operation of signal processing devices of SRR. The influence of these signal distortions is especially strong manifested in the case of the autodyne oscillator interaction with radiation reflected from the distributed object [15].

A large number of publications are devoted to studying of distortion problem of autodyne signals in various self-oscillating systems and to searching of struggle methods against them. Among proposed methods, the approaches based on using of bi-harmonic oscillator with frequency stabilization on the second harmonic [16] and autodyne oscillators with external and mutual synchronization [17] are especially effective. However, the most effective solution of this problem can be achieved at application in autodyne oscillators of the external high-*Q* cavity [18]. Frequency stabilization with the help of this cavity essentially decreases the signal distortion level and improves the radiation spectrum of UHF oscillator, which significantly increases performance and operating characteristics of autodyne SRR.

However, when the level of reflected radiation exceeds the definite quantity, the signal distortions appear in the stabilized autodyne as well, and they are caused by autodyne frequency variations. The appearance of these distortions is connected not only with the phase shift irregularity, although in the most cases they can be very small. As it is shown in [19], the key reason of mentioned distortion appearance is caused by internal properties of the oscillator itself. In this case at autodyne variations of oscillation frequency, the additional amplitude modulation on the non-linearity of the fre-

quency-dependent active conductance of the oscillation system occurs. This modulation superimposed to natural autodyne variation of the oscillation amplitude caused by the phase variations of the reflected radiation, stimulates additional signal distortions.

The purpose of this paper is the development of the most important results of further investigations of the stabilized self-oscillation system (described in [19]) for the practically interesting case of the large signal, when the reflected radiation amplitude is commensurable with the natural oscillation amplitude. In this case, at distortion analysis in the stabilized oscillator, it is necessary to take into consideration a non-linearity of the reactive part of conductance of the oscillation system besides the non-linearity of the frequency function of its active component. The analysis of such a case is connected with the use of numerical methods for the solution of the problem on the basis of the developed mathematical model of an autodyne oscillator.

## The mathematical model of autodyne oscillator for large reflected signal

The offered mathematical model is called upon to take into consideration internal parameters and key construction features of stabilized autodyne UHF oscillators. To obtain equations that are the basis of this model and describe the autodyne response formation under conditions of large reflected signals, we use an equivalent circuit and analysis results obtained in [19]. Equation (3) from this paper for conductance $Y_L(t,\tau)$ of the external oscillator load describing also the effect of the reflected radiation on the autodyne can be rewritten taking into account (2) from [19] in the form:

$$Y_L(t,\tau) = G_L(t,\tau) + jB_L(t,\tau); \qquad (1)$$

$$G_L(t,\tau) = \frac{G_L[1-\Gamma(t,\tau)^2]}{1+\Gamma^2(t,\tau)+2\Gamma(t,\tau)\cos\delta(t,\tau)};$$

$$B_L(t,\tau) = \frac{2G_L\Gamma(t,\tau)\sin\delta(t,\tau)}{1+\Gamma^2(t,\tau)+2\Gamma(t,\tau)\cos\delta(t,\tau)},$$

where $\Gamma(t,\tau) = \Gamma[A(t,\tau)/A(t)]$, $\delta(t,\tau) = \Psi(t) - \Psi(t,\tau)$ are the modulus and the phase of the instantaneous reflection factor; $A(t)$, $A(t,\tau)$ and $\Psi(t)$, $\Psi(t,\tau)$ are amplitudes and phases of the voltage on the load $Y_L(t,\tau)$, creating by the oscillator in the current time moment $t$ and in the moment $t-\tau$ from the system prehistory, relatively; $G_L$ is the external load conductance of the autonomous oscillator in which $\Gamma(t,\tau) = 0$. Here, the $\Gamma$ quantity characterizes the radiation decay at its propagation to the object and back; $\delta(t,\tau)$ is the full phase shift of the reflected wave during time $\tau = 2s/c$ of radiation propagation to reflecting object and back; $s$ is the distance to the reflector; $c$ is a velocity of radiation propagation.

Then equations (8), (9) from [19] for the conductance $Y_\Sigma = G_\Sigma + jB_\Sigma$ reduced to the active element (AE) section can be presented in the form taking into account (1):

$$G_\Sigma = \bar{G}_e + G_1 + G_1\frac{\beta_1(1+\beta_2+4Q_{c2}^2v_{c2}^2)}{(1+\beta_2)^2+4Q_{c2}^2v_{c2}^2} + \\ +2G_1\Gamma(t,\tau)\eta g_L(t,\tau) = 0; \qquad (2)$$

$$B_\Sigma = \bar{B}_e + 2G_1Q_{L1}v_{c1} + \frac{2G_1\beta_1\beta_2Q_{c2}v_{c2}}{(1+\beta_2)^2+4Q_{c2}^2v_{c2}^2} + \\ +2G_1\Gamma(t,\tau)\eta b_L(t,\tau) = 0, \qquad (3)$$

where $\bar{G}_e$ and $\bar{B}_e$ are averaged over the oscillation period active and reactive parts of the complex AE conductance depending upon the bias voltage $E$, amplitude $A$ and frequency $\omega$ of oscillations: $\bar{Y}_e(E,A,\omega) = \bar{G}_e(E,A,\omega) + j\bar{B}_e(E,A,\omega)$; $G_1 = G_{r1} + G_L$; $G_{r1}$ is the intrinsic loss of the main cavity; $\eta = G_L/G_1 = Q_{L1}/Q_{ex}$ is the efficiency of the main cavity; $Q_{L1}$, $Q_{ex}$ are its loaded and external $Q$-factors; $\beta_1$, $\beta_2$ are coupling coefficients of the main and stabilizing cavities with the transmission line between them [19]; $v_{c1}$, $v_{c2}$ are relative offsets of current frequencies of the first and second (stabilizing) cavities having the natural frequencies $\omega_{c1}$, $\omega_{c2}$ and intrinsic $Q$-factors $Q_{c1}$ and $Q_{c2}$; $g_L(t,\tau)$, $b_L(t,\tau)$ are normalized variations of the active and reactive load conductance in the vicinity of the steady-state oscillator mode:

$$g_L(t,\tau) = -\frac{\Gamma(t,\tau)+\cos\delta(t,\tau)}{1+\Gamma(t,\tau)^2+2\Gamma(t,\tau)\cos\delta(t,\tau)}; \qquad (4)$$

$$b_L(t,\tau) = \frac{\sin\delta(t,\tau)}{1+\Gamma(t,\tau)^2+2\Gamma(t,\tau)\cos\delta(t,\tau)}. \qquad (5)$$

To simplify the analysis of equation system (2), (3), we substitute the nonlinear terms of the electronic conductance $\bar{Y}_e = \bar{G}_e + j\bar{B}_e$ by its quasi-linear approximations in the vicinity of the steady-state oscillation mode. At analysis, we take into consideration that components of the conductance $\bar{Y}_e$ are the slower frequency $\omega$ functions than the oscillation system conductance. We shall express the processes occurring in the oscillator as functions of the effect of the reflected radiation level in normalized (dimensionless) values of oscillation parameter variations with respect to the steady-state mode. We limit our research to the case of autodyne response extraction of variations of oscillation amplitude by external detector at fixed AE bias voltage: $E = E_0$.

Following the stated analysis logic, we expand functions $\overline{G}_e$ and $\overline{B}_e$ in the system (2), (3) into Taylor series in the vicinity of the steady-state mode of the autonomous oscillator. Taking into consideration the closeness of frequencies $\omega_{c1}$ and $\omega_{c2}$ to the steady-state frequency $\omega_0$, we present oscillation amplitude and frequency in the form: $A = A_0 + \Delta A$; $\omega = \omega_0 + \Delta\omega$, where $\Delta E$, $\Delta A$, $\Delta\omega$ are the appropriate variations of steady-state parameters. As a result, we obtain the system of linearized equations to determine the relative variations of oscillation amplitude $a_1 = \Delta A/A_0$ and frequency $\chi = \Delta\omega/\omega_0$:

$$\alpha_{11} a_1 + \varepsilon_{11}\chi + g_{os}(\chi) + \Gamma(t,\tau)\eta g_L(t,\tau) = 0; \qquad (6)$$

$$\beta_{11} a_1 + \xi_{11}\chi + b_{os}(\chi) + \Gamma(t,\tau)\eta b_L(t,\tau) = 0, \qquad (7)$$

where $\alpha_{11} = (A_0/2\overline{G}_{e0})(\partial\overline{G}_e/\partial A)$ is the reduced slope of the oscillator increment defining the regeneration degree and the strength of its limit cycle; $\varepsilon_{11} = (\omega_0/2\overline{G}_{e0})(\partial\overline{G}_e/\partial\omega)$ is the parameter of oscillator's non-isodromic properties or the influence factor of frequency variations onto the oscillation amplitude; $\beta_{11} = (A_0/2\overline{B}_{e0})(\partial\overline{B}_e/\partial A)\tan\Theta$ is the parameter of anisochronous property; $\xi_{11} = -(\omega_0/2\overline{B}_{e0})(\partial\overline{B}_e/\partial\omega)\tan\Theta$ is the parameter of frequency stabilization taking into account the frequency slope of the reactive AE conductance; $g_{os}(\chi)$, $b_{os}(\chi)$ are normalized variations of oscillation system conductance in the vicinity of the steady-state mode:

$$g_{os}(\chi) = \frac{\beta_1}{2}\frac{(1+\beta_2)+(2Q_{c2}\chi+\vartheta)^2}{(1+\beta_2)^2+(2Q_{c2}\chi+\vartheta)^2} - \frac{\beta_1}{2}\frac{(1+\beta_2)+\vartheta^2}{(1+\beta_2)^2+\vartheta^2}; \qquad (8)$$

$$b_{os}(\chi) = Q_{L1}\chi + \frac{1}{2}\frac{\beta_1\beta_2(2Q_{c2}\chi+\vartheta)}{(1+\beta_2)^2+(2Q_{c2}\chi+\vartheta)^2} - \frac{1}{2}\frac{\beta_1\beta_2\vartheta}{(1+\beta_2)^2+\vartheta^2}, \qquad (9)$$

where $\vartheta = \nu_{02}/\nu_{bv}$ is the normalized frequency offset of the stabilizing cavity with respect to its boundary value $\nu_{bv} = 1/2Q_{c2}$; $\nu_{02} = (\omega_0 - \omega_{c2})/\omega_{c2}$ is the relative offset of the natural frequency $\omega_{c2}$ of the second cavity with respect to steady-state frequency $\omega_0$ of the autonomous oscillator. We shall call as isodromic the self-oscillator, in which the oscillation amplitude does not depend upon the oscillation frequency variations. We assume the presence of this dependence in the non-isodromous oscillator. Differential AE parameters $\alpha_{11}$, $\varepsilon_{11}$, $\beta_{11}$ and $\xi_{11}$ in (6), (7) can be calculated for the specific oscillator implementation or determined experimentally.

The obtained system of equations (6), (7) describes steady-state values and quasi-static variations of amplitude and frequency of autodyne oscillators for all values of reflected radiation levels and for arbitrary value of its delay time. It should be noted that at the absence of stabilizing cavity coupling when $\beta_1 = 0$ these equations correspond to the case of single-tank autodyne [10].

Under relevant SRR functioning conditions, the large level of reflected radiation commensurable with amplitude of natural oscillations is observed at comparably small distances to the reflector. At that, in spite of considerable parameter variations, it is quite acceptable to expand the parameters of delayed effect $\Gamma(t,\tau)$ and $\delta(t,\tau)$ in Taylor series on the small delay time $\tau$ compared to the current time $t$ ($\tau << t$ [10]) in order to simplify the further analysis of the steady-state autodyne response.

Restricting by two first expansion terms, we obtain the first approximation solution for the modulus and phase of the reflection factor in the form: $\Gamma(t,\tau) = \Gamma$; $\delta(t,\tau) = \omega\tau$.

Taking into consideration this expansion, we obtain mathematical expressions necessary for the further numerical analysis of the autodyne oscillator. Having excepted from equation (6) the variable $\chi$ and from equation (7) the variable $a_1$ and assuming in them $\eta = 1$, we obtain:

$$a_1/K_a + g_{osr}(\chi) + \Gamma g_{Lr}(\tau_d) = 0; \qquad (10)$$

$$\chi/L_a + b_{osr}(\chi) + \Gamma b_{Lr}(\tau_d) = 0, \qquad (11)$$

where $K_a = 1/\alpha_{11}(1-\gamma\rho)$ is the autodyne amplification factor; $L_a = 1/\xi_{11}(1-\gamma\rho)$ is the frequency deviation factor; $g_{osr}(\chi) = g_{os}(\chi) - \rho b_{os}(\chi)$, $b_{osr}(\chi) = b_{os}(\chi) - \gamma \times g_{os}(\chi)$ are relative active and reactive conductances of the oscillating system; $g_{Lr}(\tau_d) = g_L(\tau_d) - \rho b_L(\tau_d)$, $b_{Lr}(\tau_d) = b_L(\tau_d) - \gamma g_L(\tau_d)$ are relative active and reactive load conductances; $\gamma = \beta_{11}/\alpha_{11}$, $\rho = \varepsilon_{11}/\xi_{11}$ are non-isochronous and non-isodromous factors of the oscillator.

At that, taking into account (10) and (11) the equation for phase $\delta(t,\tau)$ including into equations (4), (5) for derivative calculation $g_{Lr}(\tau_d)$ and $b_{Lr}(\tau_d)$ can be written as:

$$\delta(t,\tau) = \delta(\chi,\tau_d) = 2\pi(1+\chi)(N+\tau_d), \qquad (12)$$

where $N = 2s/\lambda$ is the integer of half-wavelength being packed between the reflecting object and the autodyne; $\tau_d = \omega_0\tau/2\pi$ is normalized (dimensionless) time.

The solution of equation system (10), (11) provides a possibility of analysis of the autodyne response formation features on variation of the amplitude $a_1$ and the frequency $\chi$ oscillations at $\tau_d$ changing on the separate parts of the distance $s$ to the reflector.

## Effect of the oscillation system and the oscillator load upon the process of autodyne response formation

A main point of the autodyne effect consists in oscillator reaction on the influence of the proper reflected radiation, which is equivalent to variation of the load that moved away on the definite distance. These variations introduce the active and reactive conductances into oscillating system that leads to variations of the oscillation amplitude and phase. In the case of small reflected radiation, the amplitude of quasi-harmonic autodyne response is usually proportional to the reflected radiation level. However, at large reflected radiation level such a proportionality of the response is disturbed. Moreover, oscillating system characteristics and AE parameters as well as the value of distance to reflecting object affect the process of response formation.

The analysis of equations (10), (11) taking into consideration (4), (5) and (8), (9) allows clarification of the mentioned factor influence upon features of the autodyne response formation. At that, we provide investigations without taking into account the delay time value of the reflected radiation supposing in (12) $N = 0$.

At first, we consider a behavior of relative conductance components $g_{osr}(\chi)$ and $b_{osr}(\chi)$ of the oscillating system with respect to relative frequency variations $\chi$ in the vicinity of the steady-state oscillation mode. After that, we consider the response formation process itself, which as it follows from (10)–(11) is determined by a behavior of relative load conductance components $g_{Lr}(\tau_d)$ and $b_{Lr}(\tau_d)$ depending on relative variations of dimensionless time $\tau_d$ taking into account the introduced by AE parameters of non-isochronous $\gamma$ and non-isodromous $\rho$ properties of the autodyne.

In the further analysis, we consider the matching condition for transmission line with the stabilizing cavity, at which $\beta_2 = 1$. We determine the frequency functions of normalized conductances $g_{osr}(\chi)$ and $b_{osr}(\chi)$ assuming the different values of the $\beta_1$ parameter determining the cavity coupling degree at variations of non-isochronous $\gamma$ and non-isodromous $\rho$ features of the oscillator, which characterize its intrinsic properties. Calculation results according to (10) and (11) taking into account (8) and (9) for $Q_{L1} = 100$, $Q_{c2} = 1000$ and $\vartheta = 0$ in the form of graphs of frequency functions of normalized conductance $g_{osr}(\chi)$ and $b_{osr}(\chi)$ are presented in Fig. 1. We would like to note here that curves *1* show characteristics corresponding to the case of the autodyne with the single-tank oscillation system, at which $\beta_1 = 0$.

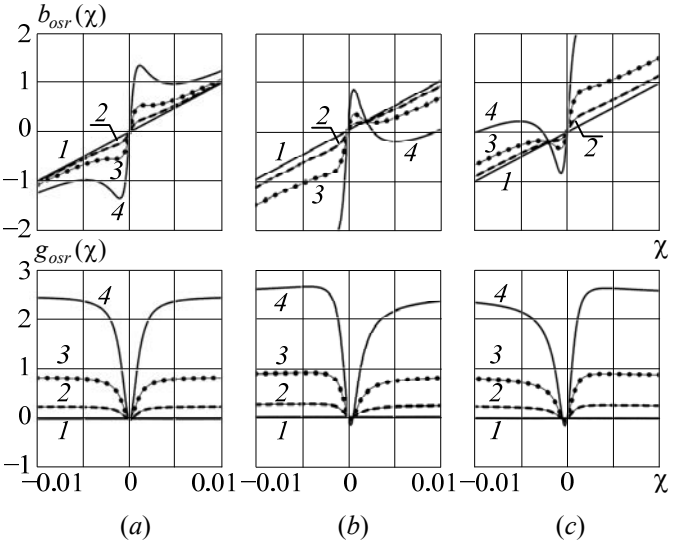


Fig. 1. Normalized characteristics of frequency functions of reactive $b_{osr}(\chi)$ and active $g_{osr}(\chi)$ components of oscillation system calculated at different values of parameter $\beta_1$: $\beta_1 = 0$ (curves *1*); $\beta_1 = 1$ (curves *2*); $\beta_1 = 3.4$ (curves *3*); $\beta_1 = 10$ (curves *4*) and factors $\gamma$ and $\rho$: (*a*) $\gamma = \rho = 0$; (*b*) $\gamma = \rho = 0.5$; (*c*) $\gamma = \rho = -0.5$.

The analysis of graphs for the case of the isochronous and isodromous oscillator $\gamma = \rho = 0$ shown in Fig. 1*a* proves that under condition of the exact tuning of the stabilized cavity (when $\vartheta = 0$) characteristics of the frequency functions of the reactive $b_{osr}(\chi)$ component of the oscillating system conductance have a central symmetry, while characteristics of the active component $g_{osr}(\chi)$ have the axial symmetry. At that, if the $\beta_1$ parameter does not exceed the critical value of coupling between cavities ($\beta_1 \le \beta_{cc}$), which is equal $\beta_{cc} = 3.4$ in the considered case ($Q_{c2} = 1000$), then characteristics $b_{osr}(\chi)$ are one-valued functions of frequency as curves *1*–*3* demonstrate. It follows from curves *4* that at value of $\beta_1$ parameter exceeding the critical value, the "bending deflections" appear in these characteristics, which was noted in [19]. Segments of these characteristics, where derivatives have the negative sign, correspond to unstable operation [20].

In the case when $\beta_1 \le \beta_{cc}$, the operation point on characteristics $b_{osr}(\chi)$ for autodyne frequency variations moves along the continuous trajectory. If this inequality does not fulfil, the qualitatively another situation is observed in the operation point movement. In this case, the operation point on these characteristics bypasses unstable segments with a negative derivative

by the jump with hysteresis phenomena. Calculations show that the critical coupling value $\beta_1 = \beta_{cc}$ takes another one at the variation of $Q_{c2}$. We consider this value of the coupling parameter $\beta_{cc}$ as the boundary value between cases of large $(\beta_1 > \beta_{cc})$ and small $(\beta_1 < \beta_{cc})$ coupling between cavities since it determines qualitative differences in the character of autodyne frequency variations.

The sharp dip presence in the characteristic $g_{osr}(\chi)$ indicates the abrupt increase of the active conductance during autodyne variations of generation frequency with respect to $\chi = 0$. At that, the additional amplitude modulation with doubled frequency occurs. As it was proved in [19], this phenomenon is a reason of autodyne oscillator non-linearity on amplitude.

The similar characteristics for the case, when AE introduces the additional dependence of the reactive $b_{osr}(\chi)$ and active $g_{osr}(\chi)$ components of the conductance on amplitude variations (non-isochronous property) and on frequency variations (non-isodromous property) into the resonance system are shown in Fig. 1*b* and Fig. 1*c*. As can be seen from these graphs, in this case the central and axial symmetry of characteristics are observed. Due to oscillator non-isochronous property $(\gamma \neq 0)$ and introduction of the component of the active conductance $\gamma g_{os}(\chi)$ into the reactive conductance $b_{osr}(\chi)$, the characteristics $b_{osr}(\chi)$ receive the frequency offset $\chi$ in the form of bending deflection for the single sign, while for another sign it is observed their flattening. A behavior of characteristics $g_{osr}(\chi)$ is specified by the introduction of the quantity $\rho b_{os}(\chi)$ into the conductance $g_{os}(\chi)$ due to non-isodromous property $(\rho \neq 0)$ of the oscillator. Owing to this, the slope and descent height of the characteristic $g_{osr}(\chi)$ are changed. Mentioned peculiarities of characteristics $g_{osr}(\chi)$ and $b_{osr}(\chi)$ essentially influence the autodyne response formation at the large reflected signal.

Fig. 2 shows diagrams calculated according to (10), (11), which illustrate the process of autodyne response formation for the case of the isochronous and isodromous oscillator $(\gamma = \rho = 0)$. The diagram sequence numbers are shown by figures in the low right corner, the functional direction of conversion processes is indicated by arrows, the sign "+" means its summation. Let us consider the autodyne response formation process itself using diagrams shown in Fig. 2. As the probing signal, we take sinusoidal variations of the reactive and active load conductances of unit amplitude: $b_{Lr}(\tau_d) = b_L(\tau_d) = \sin 2\pi\tau_d$; $g_{Lr}(\tau_d) = g_L(\tau_d) = -\cos 2\pi\tau_d$ shown in diagrams 1 and 6. We assume that the parameter $\beta_1$ is equal to its boundary value $\beta_1 = 3.4$.

As follows from (11) and the diagram 2, the conductance $b_{Lr}(\tau_d)$ leads to displacement of the characteristic $b_{osr}(\chi)$ along ordinate axis: $b_{osr}(\chi) + b_{Lr}(\tau_d)$. At that, intersect points of the characteristic and abscissa axis give the current values of the autodyne response on the frequency variations $\chi(\tau_d)$, which is called as the frequency characteristic of autodyne (FCA) in the autodyne theory. As can be seen from the diagram 3, these variations $\chi(\tau_d)$ are inverted with respect to the input impact $b_{Lr}(\tau_d)$.

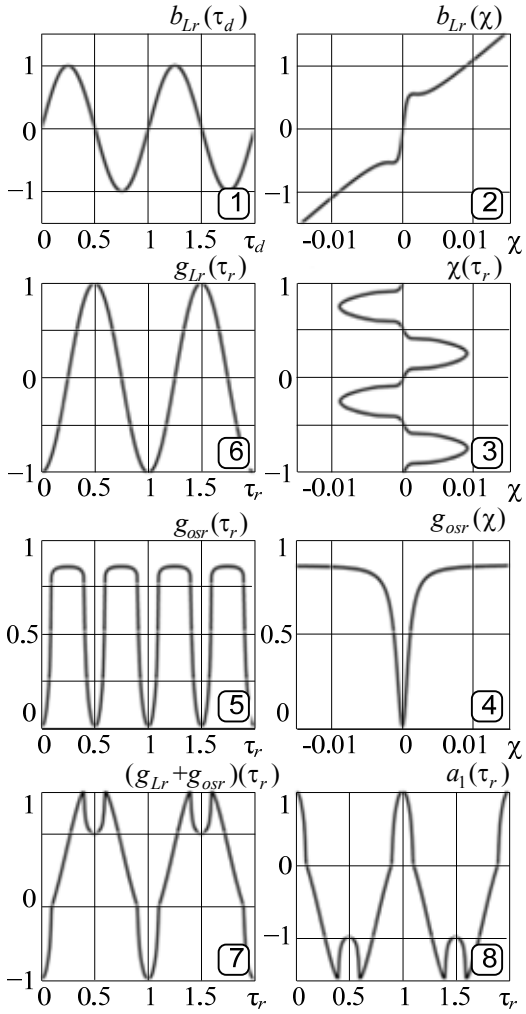


Fig. 2. Diagrams of the process of autodyne response formation for the stabilized isochronous oscillator for the large reflected signal.

The slope of the central part of the characteristic $b_{Lr}(\tau_d)$ shown in the diagram 2 reflects the stabilizing cavity action. It is equal to the equivalent *Q*-factor $Q_{equ}$ of the oscillating system under consideration

$$Q_{equ} = \omega_0 \left( \frac{db_{osr}(\omega)}{d\omega} \right)_0 = Q_{L1} + \frac{\beta_1 \beta_2}{(1+\beta_2)^2} Q_{c2} .$$

Beyond the limits of the central part, where the inequality $Q_{L1} << Q_{equ}$ is fulfilled, the slope of this characteristic is determined by the *Q*-factor of the main cavity $Q_{L1}$. Therefore, the fixing capability on frequency of the oscillating system for small variations of the conductance $b_{Lr}(\tau_d)$ is higher than for the large deviations of $b_{Lr}(\tau_d)$. This explains the presence of breaking in frequency response curve $\chi(\tau_d)$ in the diagram 3.

Autodyne frequency variations $\chi(\tau_d)$ formed in accordance with the diagram 3 cause the operating point displacement along the characteristic $g_{osr}(\chi)$, as it is shown in the diagram 4. At that, the current variations of the conductance $g_{osr}(\chi)$ occur with the doubled frequency, which is illustrated by the diagram 5. A sum of the harmonic variations of the active conductance $g_{Lr}(\tau_d) = g_L(\tau_d) = -\cos 2\pi\tau_d$ and caused variations of the conductance $g_{osr}(\tau_d)$, shown respectively in diagrams 6 and 5, gives a law of variations of the resultant conductance $g_{osr}(\tau_d) + g_{Lr}(\tau_d)$, presented in diagram 7. Inversion of this law in accordance with (10) at limit cycle fastness $\alpha_{11} = 1$ gives the autodyne response $a_1(\tau_d)$ on amplitude variations (the diagram 8) for considered oscillating system, which is accepted to call as the amplitude characteristic of the autodyne (ACA) in the autodyne theory. As follows from diagrams 3 and 8, due to non-linearity of the frequency functions of active $g_{os}(\chi)$ and reactive $b_{os}(\chi)$ conductances of the oscillating system, the stabilized oscillator response is far enough from the sinusoidal form even in the hypothetic case of sinusoidal variations of the load conductances $g_{Lr}(\tau_d)$ and $b_{Lr}(\tau_d)$.

As follows from (4) and (5), under conditions of the large reflected signal, when the reflection factor value is closed to 1, both the active $g_{Lr}(\tau_d)$ and the reactive $b_{Lr}(\tau_d)$ components of the load conductance shown in diagrams 1 and 6 in Fig. 2 are also non-sinusoidal functions of the delay time. Calculation results of these characteristics for different values of the reflection factor modulus $\Gamma$, coefficients of non-isochronous property $\gamma$ and non-isodromous property $\rho$ are presented in Fig. 3. Fig. 4 shows the harmonic coefficients of reactive $K_b$ and active $K_g$ conductances as well as levels of first five harmonics of reactive $b_{Lr}(n)$ and active $g_{Lr}(n)$ conductances versus the reflection factor modulus value $\Gamma$. On these graphs and later $n = 1, 2, ..., 5$ is the harmonic sequence number; $F_d = 1/T_d$ is the normalized period of conductance variations; $T_d = 1$ is the normalized period of the autodyne response.

The analysis of graphs presented in Fig. 3 shows that the variations of reactive $b_{Lr}(\tau_d)$ and active $g_{Lr}(\tau_d)$ conductances are sinusoidal for the small reflected radiation level, when $\Gamma < 0.1$. The non-isochronous and non-isodromous properties of the oscillator cause the relative phase shifts of these conductances only. It follows from (10), (11) taking into consideration (4), (5) and graphs of Fig. 3*a* that in the case of isochronous and isodromous oscillator $g_{Lr}(\tau_d)$ is the even function of $\tau_d$, and $b_{Lr}(\tau_d)$ is the odd function. It means that at changing of the reflector displacement direction (the sign of $\tau_d$), the type of graphs $g_{Lr}(\tau_d)$ is not changed, while graphs $b_{Lr}(\tau_d)$ are rotated mirror-like with respect to abscissa axis. At noticeable characteristic distortions when $\Gamma > 0.1$, the order of sequence of gentle and steep parts of the function $b_{Lr}(\tau_d)$ is reversed at variation of $\tau_d$. As follows from curves *2* shown in Fig. 3*a* and Fig. 3*b*, at large reflected signal, the sign reverse of the coefficient $\gamma$ of characteristics $b_{Lr}(\tau_d)$ of the non-isochronous oscillator ($\gamma \neq 0$) changes not only the sequence order of the steep and gentle parts during variations of $\tau_d$, but the sequence polarity of sharp and flat half-waves. At variation $\tau_d$ in the case of non-isochronous oscillator ($\rho \neq 0$), the sign change of $\rho$ coefficient causes variations of the sequence order of steep and gentle parts of characteristics $g_{Lr}(\tau_d)$ only. These results allow conclusion that autodyne response distortions in the case of the large reflected signal are mainly determined by non-linearity of the load conductance but not because of signal limitations by AE electronic conductance as it was supposed in [21]. Therefore, the linear approximation of active $\overline{G}_e$ and reactive $\overline{B}_e$ parts of conductance assuming in equations (6) and (7) seems to be quite correct.

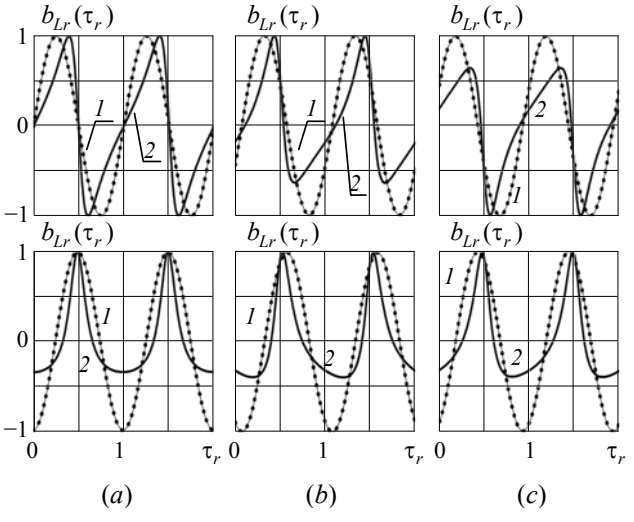


Fig. 3. Normalized reactive $b_{Lr}(\tau_d)$ and active $g_{Lr}(\tau_d)$ load conductances versus normalized time $\tau_d$ calculated at $\Gamma = 0.01$ (curves *1*) and $\Gamma = 0.5$ (curves *2*) for different values of coefficients $\gamma$ and $\rho$: (*a*) $\gamma = \rho = 0$; (*b*) $\gamma = -0.5$, $\rho = 0.5$; (*c*) $\gamma = 0.5$, $\rho = -0.5$.

As follows from graphs shown in Fig. 4, the dependences of harmonic coefficients $K_b$ and $K_g$ as well as harmonic components of reactive $b_{Lr}(n)$ and active $g_{Lr}(n)$ conductances have the similar character. There are slight differences only in harmonic characteristics of reactive conductance of isochronous and isodromous oscillator.

As can be seen from graphs in Fig. 4, at reflection factor modulus value $\Gamma = 0.1$ the levels of harmonic coefficients $K_b$ and $K_g$ does not exceed 10 %. Such levels of harmonics are in the limits of the measurement error and, hence, are quite acceptable for qualitative investigations of processes under consideration in the autodyne UHF oscillators. Therefore, at $\Gamma < 0.1$ the analysis of the autodyne UHF oscillators can be correctly fulfilled using the approximated equations for the load conductance [7–14].

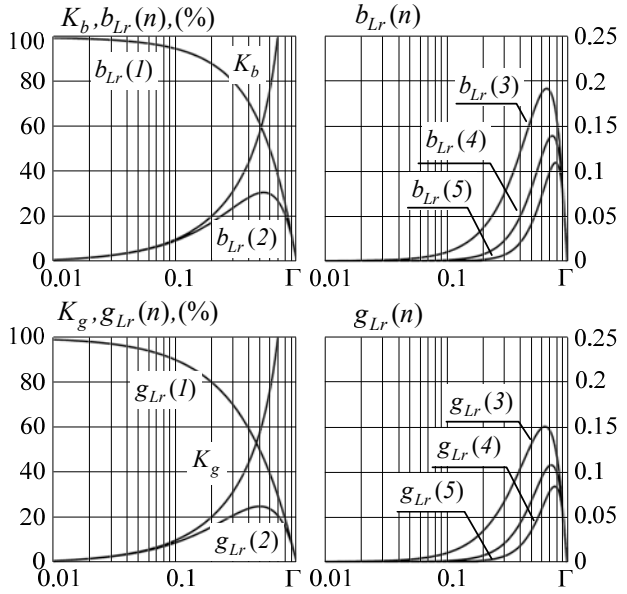


Fig. 4. Harmonic coefficients $K_b$ and $K_g$ as well as first five harmonics levels of reactive $b_{Lr}(n)$ and active $g_{Lr}(n)$ conductances versus reflection factor modulus value Γ calculated for $\gamma = \pm 1$, $\rho = \pm 0.5$.

As follows from Fig. 3 and Fig. 4, the increase of the reflection factor modulus over $\Gamma > 0.1$ is accompanied with the essential distortion growth in variation of conductances $b_{Lr}(\tau_d)$ and $g_{Lr}(\tau_d)$ as well as the sharp increase of the higher harmonic levels of these functions and essential decrease of the first harmonic components $g_{Lr}(1)$ and $b_{Lr}(1)$. In the vicinity of the value $\Gamma = 0.7$, there are the maximal higher harmonic levels, and at further reflection factor growth there is the sharp decay down to zero.

Below we describe the analysis of formation features of the autodyne signal on the basis of numerical modeling results for the case of exact cavity tuning taking into consideration intrinsic oscillator parameters, non-linearity of oscillating system and load conductances.

## Autodyne characteristics at large reflected signal

For correct application of stabilized autodyne UHF oscillators, it is important to investigate frequency $\chi(\tau_d)$ and amplitude $a_1(\tau_d)$ characteristics of the autodyne under influence of the proper reflected radiation [8–14, 19]. These characteristics normalized with respect to their maximal values provide the possibility of examination of autodyne response formation at its extraction in the form of the useful signal on amplitude variations $a_{d1}(\tau_d)$ and frequency variations $\chi_d(\tau_d)$ at variations of $\tau_d$ at separate fragments of distance $s$ to the reflector. Let us consider these characteristics for the case of extremely small distance to the reflector $(N=0)$ and exact tuning of the stabilizing cavity $(\vartheta=0)$ on the natural frequency $\omega_0$ of the autonomous oscillator.

To calculate characteristics $\chi(\tau_d)$ and $a_1(\tau_d)$ as functions of normalized time $\tau_d$, which reflect peculiarities of the oscillation system behavior at load variations, we use equations (10) and (11). We search the solution of this equation system using mathematical approach of the package Mathcad. At first, we find the autodyne frequency variations $\chi(\tau_d)$ solving the transcendent equation (11) by the secant method with the help of the iteration algorithm realized in function Root. Substituting the obtained $\chi$ values into equation (10), we obtain the subset of variable $a_1 = a_1(\tau_d)$. After that, with the help of the built-in function Maximize (f, $x_1,\ldots,x_m$), we obtain the maximal values $a_{1m}$ and $\chi_m$ of resulting functions $a_1 = a_1(\tau_d)$ and $\chi = \chi(\tau_d)$. We use these maximal values $a_{1m}$ and $\chi_m$ for the normalization of the required autodyne characteristics: FCA $a_{d1}(\tau_d) = a_1(\tau_d)/a_{1m}$ and ACA $\chi_d(\tau_d) = \chi(\tau_d)/\chi_m$. An evaluation of the analysis reliability with the developed algorithm was verified by the comparison of calculated autodyne characteristics and results obtained in [19] for the case of small reflected signal when $\Gamma << 1$.

Results of numerical investigations of autodyne characteristics are presented below for the following parameter values: $\beta_2 = 1$; $Q_{L1} = 100$; $Q_{c2} = 1000$; $\vartheta = 0$; $N = 0$; $\alpha_{11} = 1$. Fig. 5 shows FCA $\chi_d(\tau_d)$ and ACA $a_{d1}(\tau_d)$ for the cases of the small $(\Gamma = 0.01)$ and large $(\Gamma = 0.5)$ reflected signals. Fragments of these characteristics represent the types of frequency dependences of reactive $b_{osr}(\chi)$ and active $g_{osr}(\chi)$ conductances of the oscillating system. Graphs of harmonic coefficients

of frequency $K_{hf}$ and amplitude $K_{ha}$ variations as well as the harmonic component levels of autodyne response spectra on frequency variations $\chi_d(F_d)$ and amplitude variations $a_{d1}(F_d)$ versus the reflection factor modulus value $\Gamma$ of the oscillator under consideration are presented in Fig. 6.

Let us examine the results of the numerical modeling of autodyne oscillators. As follows from curves *1* shown in Fig. 5, in the case of the small reflected signal, FCA $\chi_d(\tau_d)$ and ACA $a_{d1}(\tau_d)$ have sinusoidal form. At that, variations of coefficients of non-isochronous property $\gamma$ and non-isodromous property $\rho$ cause the variations of the relative angles of the phase shifts $\theta = \arctan\gamma$ and $\psi_1 = \arctan\rho$ of the autodyne response components only. These conclusions are well coordinated with known results of the small-signal investigations of the autodyne UHF oscillators [10, 19].

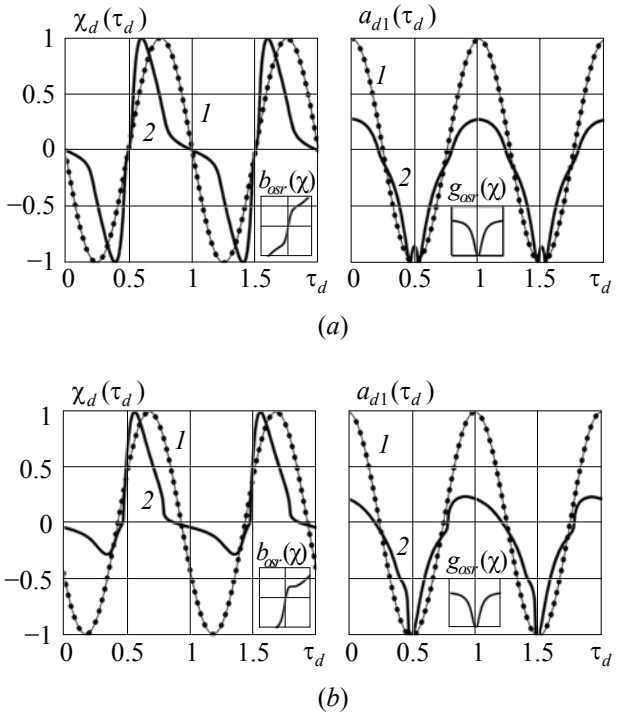


Fig. 5. FCA $\chi_d(\tau_d)$ and ACA $a_{d1}(\tau_d)$ of stabilized autodyne oscillator for $\beta_1 = 1.5$ and different values of coefficients $\gamma$ and $\rho$: (*a*) $\gamma = \rho = 0$; (*b*) $\gamma = 0.5$, $\rho = 0$. Curves *1* with dots correspond to the reflection factor modulus $\Gamma = 0.01$, solid curves *2* are presented for $\Gamma = 0.5$.

At the large reflected signal, the phase shifts of autodyne frequency variations $\chi_d(\tau_d)$ and amplitude variations $a_{d1}(\tau_d)$ depending on the values of coefficients $\gamma$ and $\rho$ occur as well, what can be well seen on the displacements of curves *2* in Fig. 5. However, to provide the efficiency of the SRR autodyne oscillators under examination for the large reflected signal, the most important problem is the search of reasons of distortion appearance of the autodyne response components.

Comparison of the results presented in Fig. 3 and Fig. 5 shows that for the same values of coefficients $\gamma$ and $\rho$, in contrast to normalized reactive $b_{Lr}(\tau_d)$ and active $g_{Lr}(\tau_d)$ load conductances, the appropriate characteristics $\chi_d(\tau_d)$ and $a_{d1}(\tau_d)$ have additional distortions caused by the oscillating system non-linearity. It follows also from Fig. 5 that the oscillator non-isochronous property affects the law of formation both FCA and ACA. At the same time, the oscillator non-isodromous property has an influence only on the form of ACA.

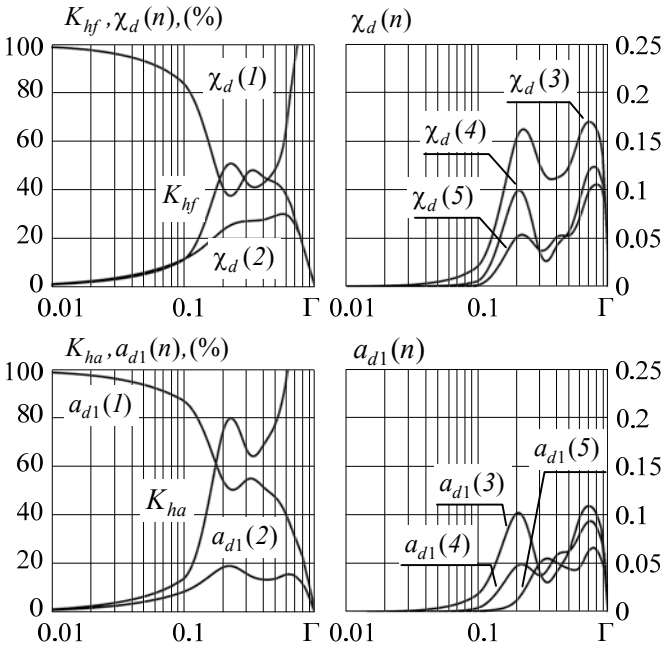


Fig. 6. The main harmonic component levels of the autodyne response spectra for the stabilized oscillator on the frequency variation $\chi_d(n)$ and on the amplitude variation $a_{d1}(n)$ as well as the harmonic coefficients $K_{hf}$ and $K_{ha}$ versus the reflection factor modulus values $\Gamma$ calculated for $\beta_1 = 1.5$ and $\gamma = \rho = 0.5$.

Comparison of frequency dependences of the reactive $b_{osr}(\chi)$ and active $g_{osr}(\chi)$ conductances of the oscillating system as well as characteristics $\chi_d(\tau_d)$ and $a_{d1}(\tau_d)$ shows that positive and negative half-waves of the autodyne response on the frequency variation $\chi_d(\tau_d)$ have the same amplitudes only in the case of the isochronous oscillator $(\gamma = 0)$, which frequency function $b_{osr}(\chi)$ has the symmetric form, as it follows from Fig. 5*a*. In the case of the non-isochronous oscillator $(\gamma \neq 0)$, the partial cut of one of the half-waves of the autodyne characteristic $\chi_d(\tau_d)$ is observed, as can be seen in Fig. 5*b*. This phenomenon and the breaking

of characteristics $\chi_d(\tau_d)$ in the range of small values of autodyne frequency variations occur due to the action of the stabilizing cavity, which tries to keep the oscillation frequency in the central part of the frequency band. Beyond the boundaries of the stabilization band, where the frequency function $b_{osr}(\chi)$ slope is determined by the $Q$-factor $Q_{L1}$ of the main cavity only, frequency variations are sharply increased causing non-symmetry appearance in the characteristic of the autodyne response.

For more complete investigation of formation process of distorted autodyne characteristics presented in Fig. 5, we examine Fig. 2 again. We replace the diagrams 1 and 6 in this figure by the appropriate diagrams of reactive $b_{Lr}(\tau_d)$ and active $g_{Lr}(\tau_d)$ load conductances presented in Fig. 3. We replace also the diagrams 2 and 4 for the same values of coefficients $\gamma$ and $\rho$ by frequency functions of reactive $b_{osr}(\chi)$ and active $g_{osr}(\chi)$ conductances of the oscillating system, which are shown in Fig. 1. Then, on diagrams 3 and 8 we obtain the appropriate graphs of autodyne frequency variations $\chi(\tau_d)$ and amplitude variations $a_1(\tau_d)$, which after normalization will have the form presented in Fig. 5 as the frequency $\chi_d(\tau_d)$ and amplitude $a_{d1}(\tau_d)$ characteristics.

Now, we compare graphs (presented in Fig. 6) of functions of the main harmonic spectra components of the autodyne response for the stabilized oscillator on the frequency variation $\chi_d(n)$ and on the amplitude variation $a_{d1}(n)$ as well as the harmonic coefficients of frequency $K_{hf}$ and amplitude $K_{ha}$ characteristics versus the reflection factor modulus value $\Gamma$ with graphs presented in Fig. 4 for the load conductance.

The results of this comparison indicate that a behavior of all characteristics on their initial segments before the reflection factor value $\Gamma = 0.1$ and on the final segment, where $\Gamma > 0.5$, is qualitatively similar. An exception is the region of $\Gamma$ variation between values from 0.1 to 0.5.

In this region, the bend of levels characteristics of the first harmonics $\chi_d(1)$ and $a_{d1}(1)$ as well as the noticeable growth of levels of the higher harmonics $\chi_d(n)$ and $a_{d1}(n)$ are observed. The non-monotone behavior of harmonic coefficient functions $K_{hf}$ and $K_{ha}$ is manifested here. In this intermediate region of $\Gamma$ value variations, the reflected signal level achieves the value corresponding to the bend point of the frequency function of the reactive conductance $b_{osr}(\chi)$ of the oscillating system. At further growth of the reflected signal level, the non-linearity component due to stabilizing cavity is decreased since formation of this part of the characteristic is mainly determined by parameters of the main cavity.

The results of investigations show that the coupling degree of the main and stabilizing cavities is one of the most important parameters, which fundamentally effect the characteristics of the whole autodyne SRR system under conditions of the large reflected signal. At weak coupling between cavities, the autodyne response of the oscillator with the stabilizing cavity for large reflected signal is subject to distortion in a greater degree than the autodyne response of the usual non-stabilized oscillator.

Therefore, the practical interest is the case of strong coupling, at which advantages of single-tank and stabilized oscillators are combined simultaneously. The results obtained by numerical examination of a number of characteristics for different values of the $\beta_1$ parameter indicate that these advantages are clearly manifested at coupling parameter value not less than 10. For the case of the isochronous oscillator $(\gamma = \rho = 0)$ at strong coupling between cavities, when $\beta_1 = 40$, the calculated FCA $\chi_d(\tau_d)$ and ACA $a_{d1}(\tau_d)$ are presented in Fig. 7.

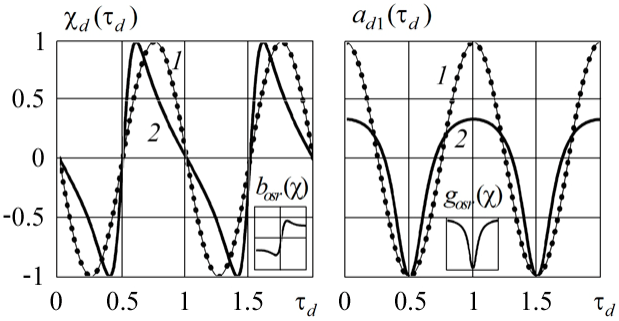


Fig. 7. FCA $\chi_d(\tau_d)$ and ACA $a_{d1}(\tau_d)$ of the stabilized autodyne oscillator with strong coupling calculated for $\beta_1 = 40$, $\gamma = \rho = 0$ and different values of the reflection factor modulus $\Gamma$: $\Gamma = 0.01$ (curves with dots) and $\Gamma = 0.5$ (solid curves).

To summarize the research results, we compare FCA $\chi_d(\tau_d)$ and ACA $a_{d1}(\tau_d)$ presented in Fig. 7 with appropriate functions of reactive $b_L(\tau_d)$ and active $g_L(\tau_d)$ load conductances (Fig. 3*a*), FCA $\chi_d(\tau_d)$ and ACA $a_{d1}(\tau_d)$ presented in Fig. 5*a*, as well as graphs of Fig. 4, Fig. 6. Results of this comparison show that in the case of strong coupling between cavities the autodyne response properties of the stabilized oscillator and the single-tank oscillator become quite similar. In this case, the autodyne characteristics are subjects to distortions in an essential lesser degree. The monotony properties of harmonic components $\chi_d(n)$, $a_{d1}(n)$ and coefficients $K_{hf}$, $K_{ha}$ dependences are observed in the range of reflection factor variation $0 < \Gamma < 0.5$.

## Conclusion

The theory of autodyne UHF oscillators stabilized by the external high-$Q$ cavity is presented under conditions of the large level of proper reflected radiation. Peculiarities of frequency and amplitude characteristic formation of the whole SRR autodyne system are studied. The distortion of the autodyne response of UHF oscillators in the case of large reflected signal is investigated. It is shown that the key reason of this distortion is non-sinusoidal form of variation of the active and active components of the complex load conductance at the uniform phase variation for the reflected wave as well as non-linearity of frequency functions of the active and reactive components of the oscillating system.

The approach of experimental researches of stabilized autodynes and their results are interesting as well for working-out recommendations concerning their practical applications in short-range radar systems.

The results obtained in this paper may be useful at development of calculation methods for stabilized autodynes interacting with the proper reflected radiation, and at optimization of UHF oscillator parameters, which are intended for autodyne SRR.

## References

1. Page C. H., Astin A. V. Survey of proximity fuze development // American Journal of Physics. – 1947. – Vol. 15, N. 2. – P. 95–110.

2. Komarov I. V., Smolskiy S. M. Fundamentals of short-range FM radar. – Norwood: Artech House, 2003. – 289 p.

3. Usanov D. A., Scripal Al. V., Scripal An. V. Physics of semiconductor RF and optical autodynes. – Saratov: Saratov University Publisher, 2003. – 312 p. [in Russian].

4. Zakarlyuk N. M., Noskov V. Ya., Smolskiy S. M. On-board autodyne velocity sensors for aeroballistics inspections // Proceedings of 20th International Crimean Conference "Microwave & Telecommunication Technology", September 13–17, 2010. – Sevastopol: Weber. – 2010. – Vol. 2. – P. 1065–1068.

5. Zakarlyuk N. M., Noskov V. Ya., Smolskiy S. M. Autodyne sensors for railway crossings // Proceedings of 20th International Crimean Conference "Microwave & Telecommunication Technology", September 13–17, 2010. – Sevastopol: Weber. – 2010. – Vol. 2. – P. 1072–1076.

6. Smolskiy S. M. Generalov M. K. Homodyne and autodyne configurations of short-range radar systems // Telecommunication Sciences. – 2010. – Vol. 1, N. 1. – P. 14–23.

7. New direction-of-motion Doppler detector / M. J. Lazarus, F. P. Pantoja, M. Somekh, at all // Electronics Letters. – 1980. – Vol. 16, N. 25. – P. 953–954.

8. General characteristics and peculiarities of the autodyne effect in oscillators / E. M. Gershenzon, B. N. Tumanov, V. T. Buzykin, at al // Radio Engineering and Electronics. – 1982. – Vol. 27, N. 1. – P. 104–112 [in Russian].

9. Votoropin S. D., Zakarlyuk N. M., Noskov V. Ya., Smolskiy S. M. On principal impossibility of autosynchronization of an autodyne by radiation reflected from a moving target // Russian Physics Journal. – 2007. – Vol. 50, N. 9. – P. 905–912.

10. Votoropin S. D., Noskov V. Ya., Smolskiy S. M. Modern hybrid-integrated autodyne oscillators of microwave and millimeter ranges and their application. Part 2. Theoretical and experimental investigations // Successes of Modern Electronic Engineering. – 2007. – N. 7. – P. 3–33 [in Russian].

11. Noskov V. Ya., Smolskiy S. M. Autodyne effect in oscillators with amplitude modulation // Radiotechnika. – 2011. – N 2. – P. 21–36 [in Russian].

12. Votoropin S. D., Noskov V. Ya., Smolskiy S. M. Analysis of autodyne effect of an RF oscillator // Russian Physics Journal. – 2008. – Vol. 51, N. 3. – P. 291–298.

13. Votoropin S. D., Noskov V. Ya., Smolskiy S. M. An analysis of the autodyne effect of oscillators with linear frequency modulation // Russian Physics Journal. – 2008. – Vol. 51, N. 6. – P. 610–618.

14. Votoropin S. D., Noskov V. Ya., Smolskiy S. M. An analysis of the autodyne effect of a radio-pulse oscillator with frequency modulation // Russian Physics Journal. – 2008. – Vol. 51, N. 7. – P. 750–759.

15. Votoropin S. D., Donskov S. V., Noskov V. Ya., Smolskiy S. M. Analysis of the autodyne signal from the distributed reflecting object // Proceedings of 17th International Crimean Conference "Microwave & Telecommunication Technology", September 10–14, 2007. – Sevastopol: Weber, 2007. – P. 744–747.

16. Noskov V. Ya. Stabilized biharmonic autodyne // Radioelectronics and Communications Systems. – 1991. – Vol. 34, N. 11. – P. 61–64 [in Russian].

17. Noskov V. Ya., Smolskiy S. M. Main features of double-diode autodynes and its application // Proceedings of 20th International Crimean Conference "Microwave & Telecommunication Technology", September 13–17, 2010. – Sevastopol: Weber, 2010. – Vol. 2. – P. 1051–1054.

18. Noskov V. Ya. Analysis of an autodyne UHF transducer for noncontact measurement and control of the dimensions of components // Measurement Techniques. – New York: Springer. – 1992. – Vol. 35, N. 3. – P. 297–301.

19. Noskov V. Ya., Ignatkov K. A., Smolskiy S. M. Analysis of signals of stabilized autodynes // Telecommunication Sciences. – 2011. – Vol. 2, N. 1. – P. 5–16.

20. Shelton E. J. Stabilization of microwave oscillations // Transactions IRE. – 1954. – Vol. ED-1, N. 4. – P. 30–40.

21. Buzykin V. T., Noskov V. Ya. Autodyne response for large reflected signal // Application of Radiowaves of Millimeter and Sub-millimeter Ranges. Collection of Scientific Papers. – Kharkov: IRE of Ukraninan Academy of Sciences. – 1992. – P. 52 – 56 [in Russian].

Received in final form October 14, 2011